

# Heat transfer analysis at hot and cold wall of a trapezoidal cavity with internal different shaped solid body

M.U. Ahammad, Salma Sultana, Tania Sultana

Department of Mathematics  
Dhaka University of Engineering and Technology (DUET), Gazipur  
Gazipur-1707, Bangladesh

**Abstract**— In this research, two-dimensional continuity, momentum and energy equations for steady state, heat transfer problem inside a trapezoidal cavity has been analyzed using Finite element method. The effect of different shaped interior heated body that may be triangle, circle or square on fluid flow and heat transfer rate at hot & cold wall has been analyzed in the present work. The investigations are performed for different values of Hartmann number ( $Ha$ ) & Grashof number ( $Gr$ ) in the range of  $50 \leq Ha \leq 200$  &  $10^2 \leq Gr \leq 10^5$ . Various results such as streamlines, isotherms and heat transfer rate at bottom and top wall in terms of the average Nusselt number are presented for considered parameters. The results point out that the average Nusselt number ( $Nu_{av}$ ) at both the heated and cold surface as well as temperature distribution of the fluid inside the domain depend significantly on the chosen three geometric configuration under implied boundary conditions. The heat transfer rate decreases with the mounting value of Hartmann number and increases with upper value of Grashof number.

**Keywords**—heat transfer, trapezoidal cavity, hot wall, cold wall, cavity

## I. INTRODUCTION

Combined natural and forced convection heat transfer problem in a trapezoidal enclosure has received extensive interest from a large number of researchers. Mixed convection induced in an open and closed cavity containing heat conducting, heat generating as well as adiabatic element on its center is significant from both theoretical and practical points of view. In modern days, such configuration frequently encounters in various engineering and industrial applications, particularly in cooling of electronic components, thermal insulation, air conditioning, heat exchangers, furnaces, chemical processing equipment and drying technologies etc. Particularly, heat transfer mechanism in cavities by natural or mixed convection is very crucial issue of research that is focused by the work of a number of authors. Sereir et al. [1] studied optimal conditions of natural and

mixed convection in a vented rectangular cavity with a sinusoidal heated wall inside with a heated solid block. An analysis of mixed convection in a differentially heated Square cavity with moving lids was carried out by Abraham and Varghes [2]. Numerical study of natural convection in square cavity with inner bodies using finite element method was presented by Pinto et al. [3]. Elsherbiny et al. [4] analyzed heat transfer in inclined air rectangular cavities with two localized heat sources. Fluid flow and heat transfer in a channel with an open cavity heated from bottom side was investigated by Timuralp and Altac [5]. Heat transfer enhancement in cavity with lid driven was reviewed by Saieed et al. [6]. Magneto-hydrodynamics free convection in the localized heat sources of an inclined trapezoidal enclosure filled with nano-fluid has been performed by Mansour et al [7]. Numerical investigation of conjugate natural convection in a cavity with a local heater by the Lattice Boltzmann method was performed by Gibanov and Sheremet [8]. Numerical simulation of natural convection in a square cavity with partially active vertical and horizontal walls was studied by Djoubair et al. [9]. Guo and Sharif [10] analyzed mixed convection in rectangular cavities at various aspect ratios with moving isothermal sidewalls and constant flux heat source on the bottom wall. Mixed convection enhancement in a rectangular cavity by triangular obstacle was presented by Afluq et al. [11]. Ibrahim and Hirpho [12] analyzed mixed convection flow in a trapezoidal cavity with non-uniform temperature using Finite element method. The author's shown that Hartman number has negative impact on the average Nusselt number whereas Richardson number has a positive effect on average Nusselt number. Zheng et al. [13] studied on natural convection heat transfer in a closed cavity with hot and cold tubes. Natural convection flow analysis has been performed by Akter and Parvin [14] in a trapezoidal cavity containing a rectangular heated body along with external oriented magnetic field.

As far the authors know the trapezoidal cavity having a centered heat conducting material (triangle, circle, square) simultaneously have not been studied yet. The goal of this work is to illustrate the flow and thermal field of the considered domain and explore variation of heat transfer at heated and cold wall of a trapezoidal cavity with different shaped inner obstacle.

## II. PROBLEM DEFINITION AND METHODOLOGY

The studied geometry of the present problem is shown in Fig. 1. The considered area of the problem is consisted by a trapezoidal cavity whose length of bottom and top wall is  $2L$  and  $L/2$  respectively with an internal heat conducting materials (triangle, circle, square). The foot wall is set at a stable temperature  $T_h$ , while the top wall maintains a low temperature  $T_c$  and rest two sides of the cavity are kept as adiabatic. A consistent magnetic field having strength  $B_0$  is imposed to the horizontal direction of left wall. All exterior and interior solid boundaries are fixed that is velocity components  $u$  and  $v$  are set to zero at four outer sides of the enclosure.

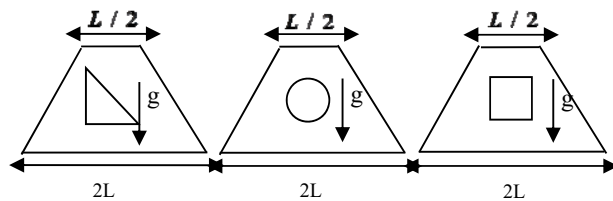


Fig. 1. The studied geometry used for numerical simulation

The cavity fluid is assumed to be two-dimensional, steady, Newtonian, laminar and incompressible. The fluid that holds constant thermo-physical properties is taken under consideration in the flow model. The buoyancy effect in the momentum equation is characterized by the Boussinesq's approximation. Also, the viscous dissipation term in the energy equation is ignored. The governing equations for the current model may be written in the dimensionless form as follows:

Continuity Equation

$$\frac{\partial U}{\partial X} + \frac{\partial V}{\partial Y} = 0 \quad (1)$$

Momentum Equation

$$U \frac{\partial U}{\partial X} + V \frac{\partial U}{\partial Y} = -\frac{\partial P}{\partial X} + \frac{1}{\text{Re}} \left( \frac{\partial^2 U}{\partial X^2} + \frac{\partial^2 U}{\partial Y^2} \right) \quad (2)$$

$$U \frac{\partial V}{\partial X} + V \frac{\partial V}{\partial Y} = -\frac{\partial P}{\partial Y} + \frac{1}{\text{Re}} \left( \frac{\partial^2 V}{\partial X^2} + \frac{\partial^2 V}{\partial Y^2} \right) + \text{Ri}\theta - \frac{\text{Ha}^2}{\text{Re}} V \quad (3)$$

Energy Equation

$$U \frac{\partial \theta}{\partial X} + V \frac{\partial \theta}{\partial Y} = \frac{1}{\text{Re Pr}} \left( \frac{\partial^2 \theta}{\partial X^2} + \frac{\partial^2 \theta}{\partial Y^2} \right) \quad (4)$$

For heat conducting solid block

$$\frac{K}{\text{Re Pr}} \left( \frac{\partial^2 \theta_s}{\partial X^2} + \frac{\partial^2 \theta_s}{\partial Y^2} \right) = 0 \quad (5)$$

Here,  $\text{Re} = \frac{u_i L}{\nu}$  is the Reynolds number,  $\text{Pr} = \frac{\nu}{\alpha}$  is the

Prandtl number,  $\text{Ha} = B_0 L \sqrt{\frac{\sigma}{\mu}}$  is the Hartmann

number,  $\text{Ri} = \frac{\text{Gr}}{\text{Re}^2}$  is the Richardson number, and

$K = \frac{k_s}{k}$  is the solid-fluid thermal conductivity ratio.

**Boundary Conditions:** The non-dimensional boundary conditions which are used in the current work can be set as follows:-

On the top wall:  $U = 0, V = 0, \theta = 0$

On the bottom wall:  $U = 0, V = 0, \theta = 1$

On the inclined walls:  $U = 0, V = 0, \frac{\partial \theta}{\partial N} = 0$

$$\left( \frac{\partial \theta}{\partial N} \right)_{\text{fluid}} = K \left( \frac{\partial \theta_s}{\partial N} \right)_{\text{solid}} \quad \text{a}$$

t the fluid-solid interfaces

The average Nusselt number  $Nu$  at the hot wall is

$$\text{given by } Nu_{\text{av}} = -\int_0^1 \left( \frac{\partial \theta}{\partial Y} \right) dX$$

### A. Method of Solution

In the present work, the solutions of the leading equations along with boundary conditions are achieved by using the finite element method. Initially, the research interest area is separated into a set of non-overlapping regions which are composed of irregular triangular elements. The coupled equations (1) - (5) are changed into a system of integral equations using Galerkin weighted residual technique and imposed proper boundary conditions. By the assist of Newton-Raphson iteration technique the non-linear algebraic equations are customized into a set of linear algebraic equations that are solved finally by means of triangular factorization method.

### B. Mesh Convergence Test

Different grid sized elements of the three configurations are taken (corresponding number of

elements are given in table 1) for the current model to check the independency of the results with the grid variations. Average Nusselt number at the bottom hot wall of the cavity are studied for these selected elements. Very minor variations are found among the results for different number of elements which is followed by Table 1.

TABLE I. GRID REFINEMENT TEST AT  $Gr = 10^4$ ,  $Ha = 50$ ,  $Re = 100$  AND  $Pr = 0.71$

Average Nusselt Number $Nu_{av}$ at Hot Wall					
Triangular body		Circular body		Squared body	
No. of elements	$Nu_{av}$	No. of elements	$Nu_{av}$	No. of elements	$Nu_{av}$
864	5.5332	621	6.3972	905	6.3810
1307	5.4221	886	6.3496	1482	6.3217
2286	5.4001	1456	6.3236	2460	6.3067
3400	5.3922	2148	6.3227	3676	6.3048
5342	5.3870	3384	6.3222	5672	6.3039

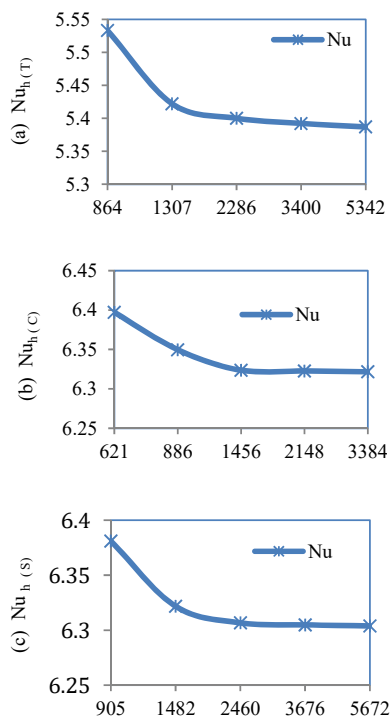


Fig. 2. Grid test shows average Nusselt number at hot and cold wall for (a) triangular (b) circular and (c) square interior body

Both the accuracy of the numerical values and the solution time throughout the simulation are taken

into account and selected the grids consisting of 3400, 2148 and 3676 elements respectively.

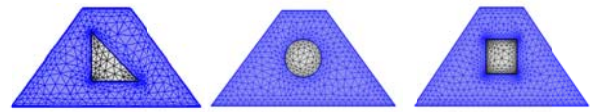


Fig. 3. Typical grid generation

### C. Code Validation

For the numerical code confirmation of the present study, a computation is carried out to compare

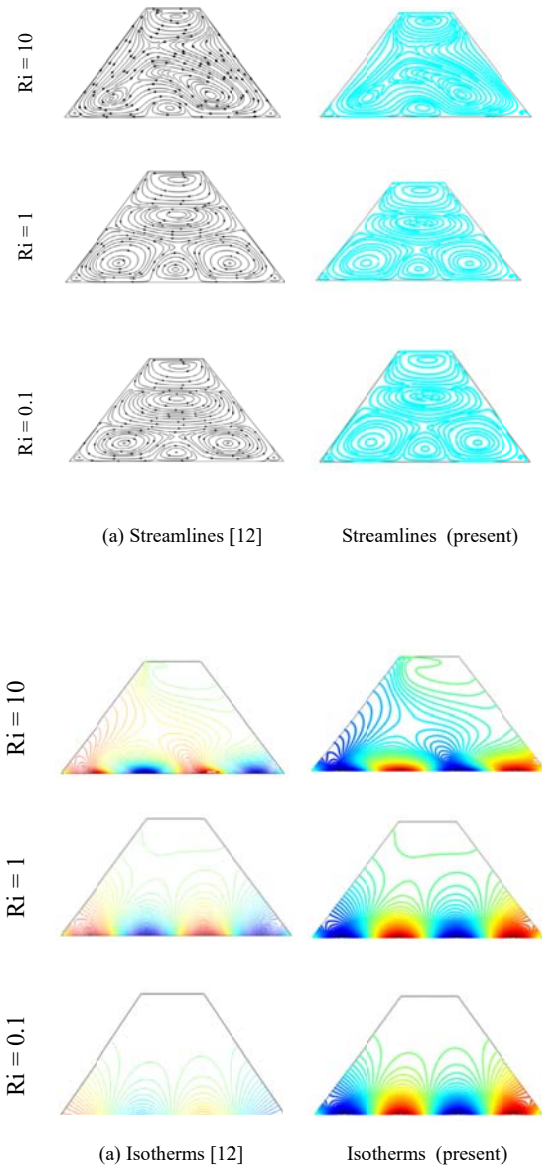


Fig. 4. Comparison of (a) streamlines and (b) isotherms while  $Gr = 10^4$ ,  $Pr = 6.2$ ,  $m = 0.25$ ,  $Ha = 50$  and  $Re = 100$

with the finite element analysis of mixed convection flow in a trapezoidal cavity with non-uniform temperature by Ibrahim and Hirpho [12]. Fig. 4 shows the relationships between the works of Ibrahim and Hirpho [12] and present with excellent agreement in streamlines and isotherms.

### III. RESULT AND DISCUSSION

The numerical computation has been carried out through the Finite element method to analyze fluid flow & heat transfer in a trapezoidal cavity heated in bottom wall and cooled in top wall containing different shaped (triangle, circle, square) inner obstacle. Effect of the pertinent parameters such as Hartman number ( $Ha$ ) and Grashof Number ( $Gr$ ) on flow and temperature field inside the cavity has been studied. The ranges of  $Ha$  and  $Gr$  for this investigation vary from  $50 \leq Ha \leq 200$  &  $10^2 \leq Gr \leq 10^5$ . The results of the present study are explained in the forms of streamlines & isotherms. In addition, the heat transfer rate both at hot and cold surface of the enclosure are shown in terms of average Nusselt Number  $Nu_h$  and  $Nu_c$  respectively.

#### Case-(i): Heat Conducting Triangular Body

The influence of Grashof number on the overall streamlines and isotherms arrangements are depicted in Fig. 5. Here the value of  $Pr$  is chosen as 0.71 which corresponds to air with  $Ha=50$ ,  $Re=100$ . These figures show the streamlines and isotherms contours for various Grashof number varied from  $10^2$  to  $10^5$ .

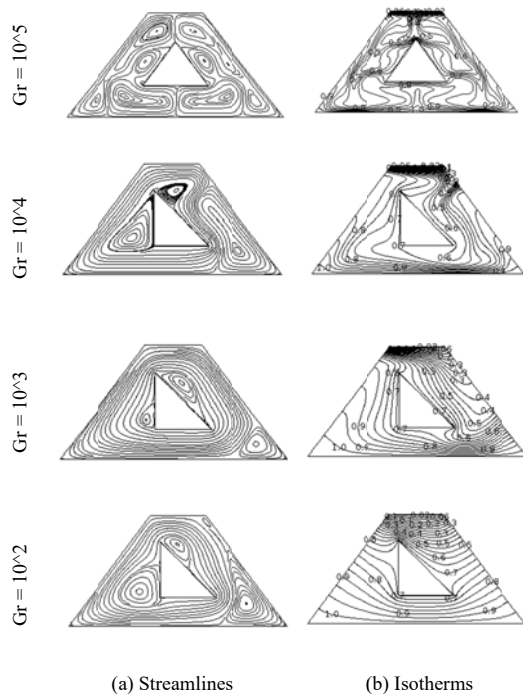


Fig. 5. Streamlines and isotherms for different values of  $Gr$  at  $Pr=0.71$ ,  $Ha=50$ ,  $Re=100$

From Fig. 5(a) it is observed that at low Grashof number  $Gr=10^2$ , a very large counter clockwise vortex is developed confining the centered triangle for  $Re=100$ , another some small vortex is found inside the enclosure of which comparatively larger vortex is formed at right bottom corner of the cavity. When  $Gr=10^3$  the small vortices reduce in size and consequently main vortex occupies the space of the domain. The overall shape of the vortices change at higher Grashof number  $Gr=10^4$  and for the largest value of  $Gr=10^5$ , it is observed that the root vortex disappears and forms many discrete vortex that varies in size and shape.

The corresponding isotherms for different Grashof numbers are displayed in Fig. 5(b). For the lower value of  $Gr=10^2$  the heat lines are stretched almost uniformly and denser enough near the top cooled surface. At  $Gr=10^3$  the heat lines become curved shape and more compact temperature distribution is followed in the vicinity of the bottom and top wall. The temperature profile is found non-uniform and scattered with too concentrated heat lines at upper surface of the cavity while  $Gr=10^4$ . For the considered highest value of  $Gr=10^5$ , it is seen that the temperature distribution changes drastically and about symmetric with the centered vertical line of the enclosure.

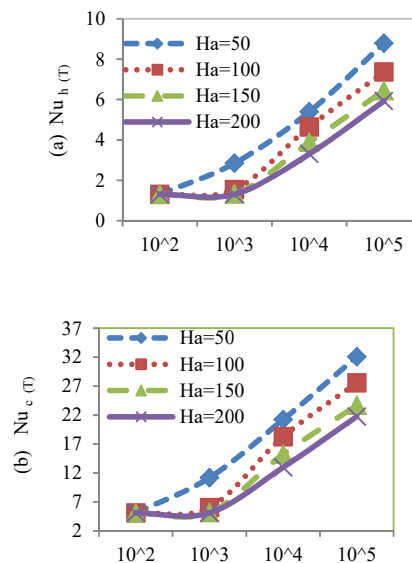


Fig. 6. Average Nusselt number at (a) hot wall and (b) cold wall versus Grashof number for different values of Hartmann number

Fig. 6 exposes the effect of Hartmann number on average Nusselt number  $Nu_{av}$  as a function of Grashof number. One can observe that the value of average Nusselt number increases as  $Gr$  increases. Also for rising values of  $Ha$ , decreasing  $Nu_{av}$  is found for all  $Ha$ . Thus the optimum heat transfer rate is recorded for the highest value of  $Gr$  along with smaller  $Ha$  and



nearly same scenario is seen for both cases of hot and cold surfaces.

### Case-(ii): Heat Conducting Circular Body

Fig. 7 describes the effect of Grashof number on the flow and temperature field for the chosen value of  $Pr=0.71$ ,  $Ha=50$  and  $Re=100$ . The streamlines seem to be symmetric about right and left half of the circle with two large rotating cells elongated from top to bottom surface for the lowest value of  $Gr=10^2$ , that is depicted in Fig. 7(a). A minor change is noticed for the rest upper values of Grashof number varied from  $10^3$  to  $10^5$ .

The isotherms for different Grashof numbers varying  $10^2 \leq Gr \leq 10^5$  are focused in Fig. 7(b). While  $Gr=10^2$ , the heat lines are distributed very homogeneously throughout the whole cavity surrounding the circular body. A smoothly curve shaped heat lines are seen and low isotherms are crowded at cold wall at  $Gr=10^3$ . For the higher values of Grashof numbers boundary layers are created near the top and bottom wall and heat lines surrounded the inner obstacle. It is also detected that while  $Gr=10^5$  isotherms are moved away towards all sides of the enclosure remarkably upper and lower surfaces.

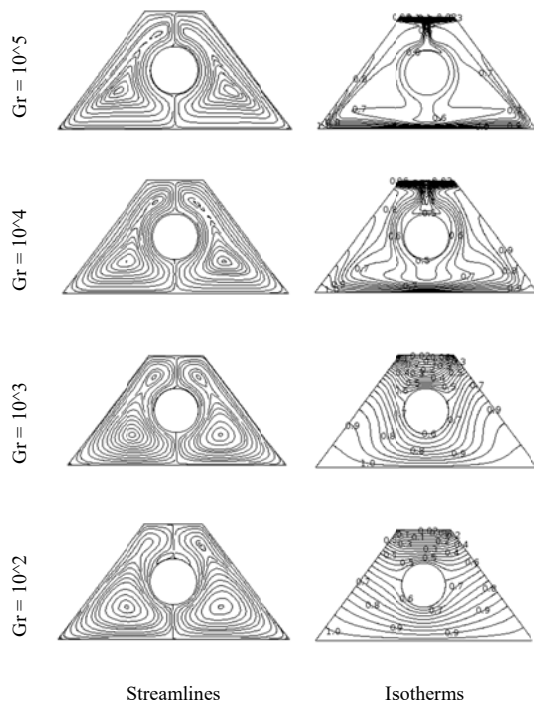


Fig. 7. Streamlines and isotherms for different values of  $Gr$  at  $Pr=0.71$ ,  $Ha=50$ ,  $Re=100$

In Fig. 8 the variation of heat transfer rate is shown in terms of average Nusselt number  $Nu_{av}$  for different values of Hartmann number versus Grashof number. It is clear that for both of heated and cooled

wall higher heat transfer rate is found when  $Gr$  increases and  $Ha$  decreases.

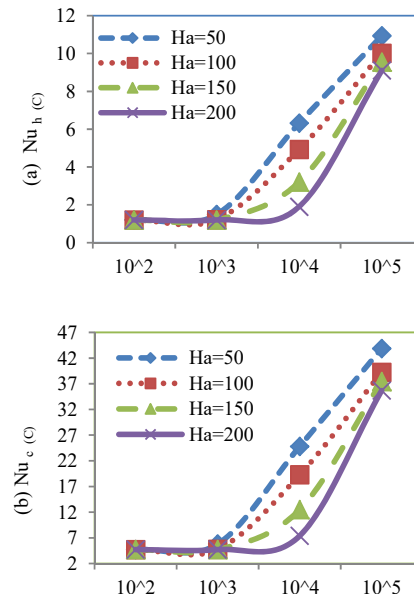


Fig. 8. Average Nusselt number at (a) hot wall and (b) cold wall versus Grashof number for different values of Hartmann number

### Case-(iii): Heat Conducting Squared Body

The streamlines and isotherms are displayed in Fig. 9 for the fixed value of  $Pr=0.71$ ,  $Ha=50$ ,  $Re=100$  and different values of Grashof number varying as  $10^2$  to  $10^5$ . The effect of Grashof number in flow field is shown in Fig. 9(a), from these figures it is noted that the streamlines are symmetric about the centered vertical line of the enclosure with two large rotating cells that encompasses the square body for all the considered values of  $Gr$ . A small variation is followed in flow patterns for the higher values of Grashof number.

In Fig. 9(b), the isotherms are displayed for different values of Grashof numbers. At  $Gr=10^2$ , the isotherms are dispersed very uniformly throughout the whole region adjacent to the square body. A well bend shaped heat lines are found and low isotherms are packed at cold wall at  $Gr=10^3$ . A dramatically change can easily be noticed in temperature profile for the rest two largest value of  $Gr$ . From the two sides of the centered body heat lines meet above the square and at the top wall. While  $Gr=10^5$  isotherms are suppressed at the ceiling and base of the enclosure.

The effect of Hartmann number on the average Nusselt number  $Nu_{av}$  along with Grashof number is focused in Fig. 10. From these figures it is seen that for both of heated and cooled wall higher heat transfer rate is found when  $Gr$  increases and  $Ha$  decreases.

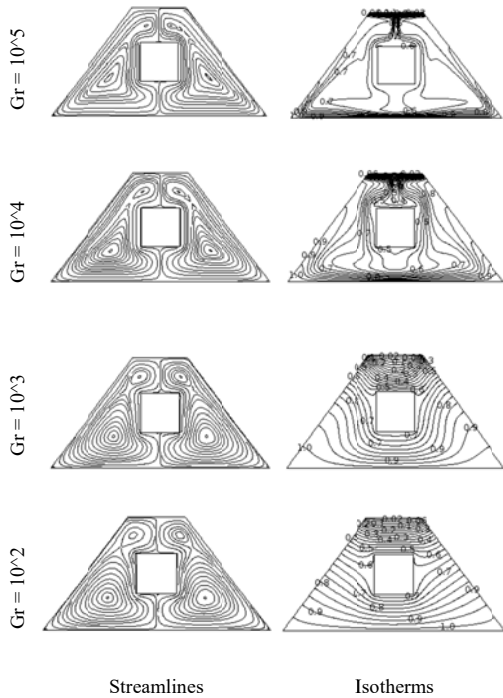


Fig. 9. Streamlines and isotherms for different values of  $Gr$  at  $Pr=71$ ,  $Ha=50$ ,  $Re=100$

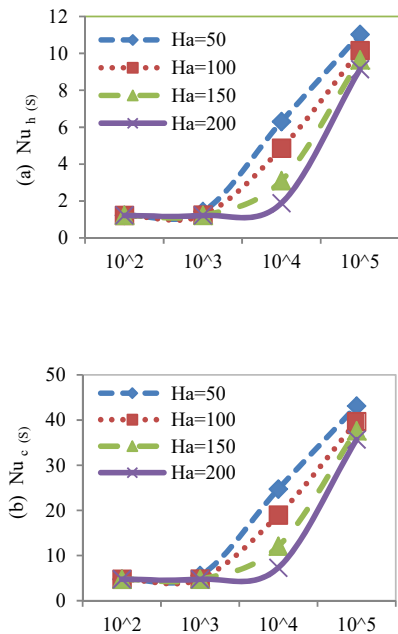


Fig. 10. Average Nusselt number at (a) hot wall and (b) cold wall versus Grashof number for different values of Hartmann number

Lastly, a comparison of rate of heat transfer at heated and cooled surface has been drawn among three different solid bodies and is shown in Fig. 11. From figure it can be conclude that triangular body gives optimum heat removal for  $.01 \leq Ri \leq .5$  whereas in  $.5 \leq Ri \leq 1$  circular body gives optimal cooling effectiveness.

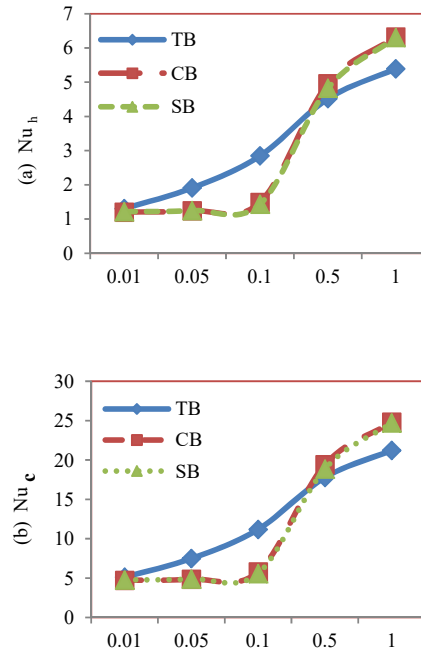


Fig. 11. Comparison of heat transfer rate at (a) hot wall and (b) cold wall among three different solid bodies along  $Ri$

#### IV. CONCLUSION

In combined, the effects of magnetic field parameter  $Ha$  and free convection parameter  $Gr$  on flow and temperature field in a trapezoidal cavity have been analyzed with internal heat conducting triangular, circular and squared body.

— A significant augmentation in heat transfer from the heated wall and cold wall is recorded due to lower values of Hartman number.

— Higher Grashof number effects in flow behaviors are more crucial in fluid flow. Heat transfer at the bottom heated surface and top cold wall increases with the increasing values of Grashof number.

— Finally, we are able to see that in triangular body (TB) the heat transfer is highest. In the circular body (CB) the heat transfer is middle and also the square body (SB) shows the lowest heat transfer.

#### REFERENCES

[1] T. Sereir, A. Missoum, B. Mebarki, M. Elmir and D. Mohamed, "Optimal conditions of natural and mixed convection in a vented rectangular cavity with a

sinusoidal heated wall inside with a heated solid block," *Wseas Transactions on Heat and Mass Transfer*, DOI: 10.37394/232012.2020.15.23, vol. 15, pp. 195-208, 2020. (validation TANIA)

[2] J. Abraham and J. Varghese, "Mixed Convection in a Differentially Heated Square Cavity with Moving Lids," *International Journal of Engineering Research & Technology* (IJERT), vol. 4, no. 12, pp. 602-607, 2015.

[3] R. J. Pinto, P. M. Guimaraes and G. J. Menon, "Numerical Study of Natural Convection in Square Cavity with Inner Bodies Using Finite Element Method," *Open Journal of Fluid Dynamics*, vol. 6, pp. 75-87, 2016.

[4] S. M. Elsherbiny, I. Osama, O. I. Ismail, Heat transfer in inclined air rectangular cavities with two localized heat sources, *Alexandria Engineering Journal*, vol. 54: p- 917-927, 2015.

[5] C. Timuralp and Z. Altac, "Investigation of fluid flow and heat transfer in a channel with an open cavity heated from bottom side," *Mugla Journal of Science and Technology*, vol. 2, no. 1, pp. 55-59, 2016.

[6] A. N. A. Saieed, M. A. S. Mustafa, S. K. Ayed and L. J. Habeeb, "Review on heat transfer enhancement in cavity with lid driven," *Journal of Mechanical Engineering Research and Developments*, vol. 43, no. 7, pp. 356-373, 2020.

[7] M. A. Mansour, A.Y. Bakier and M. A. Y. Bakeir, "MHD natural convection in the localized heat sources of an inclined trapezoidal nanofluid-filled enclosure," *American Journal of Engineering Research* (AJER), vol. 2, no. 9, pp. 140-161, 2013.

[8] N. S. Gibanov and M. A. Sheremet, "Numerical Investigation of Conjugate Natural Convection in a Cavity with a Local Heater by the Lattice Boltzmann Method," *Fluids*, 2021, 6:p316.

[9] D. Djoubair, K. Omar, C. Soufien and B. Saadoun, "Numerical Simulation of Natural Convection in a Square Cavity with Partially Active Vertical and Horizontal Walls," *IPCO*, 2014,2:

[10] G. Guo and M. A. R. Sharif, "Mixed convection in rectangular cavities at various aspect ratios with moving isothermal sidewalls and constant flux heat source on the bottom wall," *International Journal of Thermal Sciences*, vol. 43, pp. 465- 475, 2004.

[11] S. G. Afluq, M. A. A. Siba, and K. A. Jehhef, "Mixed Convection Enhancement in a Rectangular Cavity by Triangular Obstacle," *IOP Conf. Series: Materials Science and Engineering*, 2020, 881, 012083.

[12] W. Ibrahim, M. Hirpho, "Finite element analysis of mixed convection flow in a trapezoidal cavity with non-uniform temperature," *Heliyon*, <https://doi.org/10.1016/j.heliyon.2021.e05933>, vol. 6, pp.1-12, 2021.

[13] J. Zheng, L. Zhang, H. Yu, Y. Wang and T. Zhao, "Study on natural convection heat transfer in a closed cavity with hot and cold tubes," *Science Progress*, vol. 104, no.2, DOI: 10.1177/00368504211020965, pp. 1-25, 2021.

[14] A. Akter and S. Parvin, "Analysis of natural convection flow in a trapezoidal cavity containing a rectangular heated body in presence of external oriented magnetic field," *Journal of Scientific Research*, vol. 10, no.1, pp. 11-23, 2018.